ACS MATERIALS LETTERS

www.acsmaterialsletters.org

LETTER

Charting the Metal-Dependent High-Pressure Stability of Bimetallic UiO-66 Materials

Sven M. J. Rogge,* Pascal G. Yot, Jannick Jacobsen, Francesco Muniz-Miranda, Steven Vandenbrande, Jonas Gosch, Vanessa Ortiz, Ines E. Collings, Sabine Devautour-Vinot, Guillaume Maurin, Norbert Stock, and Veronique Van Speybroeck*

Cite This: *ACS Materials Lett.* 2020, 2, 438–445

Read Online

ACCESS | Metrics & More | Article Recommendations | Supporting Information

ABSTRACT: In theory, bimetallic UiO-66(Zr:Ce) and UiO-66(Zr:Hf) metal-organic frameworks (MOFs) are extremely versatile and attractive nanoporous materials as they combine the high catalytic activity of UiO-66(Ce) or UiO-66(Hf) with the outstanding stability of UiO-66(Zr). Using in situ high-pressure powder X-ray diffraction, however, we observe that this expected mechanical stability is not achieved when incorporating cerium or hafnium in UiO-66(Zr). This observation is akin to the earlier observed reduced thermal stability of UiO-66(Zr:Ce) compounds. To elucidate the atomic origin of this phenomenon, we chart the loss-of-crystallinity pressures of 22 monometallic and bimetallic UiO-66 materials and systematically isolate their intrinsic mechanical stability from their defect-induced weakening. This complementary experimental/computational approach reveals that the intrinsic mechanical stability of these bimetallic MOFs decreases nonlinearly upon cerium incorporation but remains unaffected by the zirconium:hafnium ratio. Additionally, all experimental samples suffer from defect-induced weakening, a synthesis-controlled effect that is observed to be independent of their intrinsic stability.

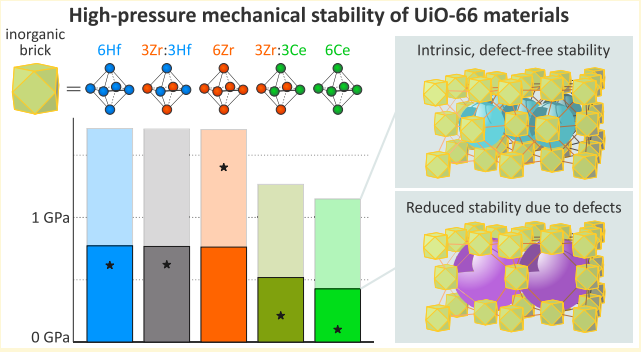

The permanent nanoporosity of metal–organic frameworks (MOFs) or porous coordination polymers makes these materials attractive for a large variety of applications.[1−7] Through the concept of reticular synthesis, this structural nanoporosity can be engineered extensively, both geometrically as well as in terms of chemical functionality, to design MOFs for targeted applications.[8−11] In the past decade, this endeavour has resulted in consciously designed MOFs that outperform competing materials in areas including gas/vapor adsorption and separation,[12−15] heterogeneous catalysis,[16,17] nanosensing,[18,19] and energy storage.[20−22] However, the porosity and rather weak coordination bonds present in MOFs also limit their mechanical, thermal, and chemical stability under operating conditions;[23,24] a stability that is typically further reduced during practical usage because of process-specific effects, such as pressure attrition.[25,26] A poor stability is prohibitive for certain synthetic or post-synthetic design strategies and shaping procedures[4,27−31] and hampers the large-scale deployment of MOFs.[29] Therefore, to bring MOF design to its full potential, it is crucial to identify to what extent the targeted incorporation of attractive functionalities in a MOF results in molecular-level alterations that impact their stability and whether the experimentally observed stability effects are intrinsic to the designed material or rather stem from the followed synthesis or activation protocol which may lead to structural defects or occluded molecules.[32,33] Herein, we systematically chart these intrinsic and synthesis-mediated stability effects for a series of monometallic and bimetallic UiO-66 materials by combining in situ high-pressure powder X-ray diffraction (PXRD) experiments with molecular dynamics (MD) simulations at operating conditions,[34,35] thereby yielding complementary insight in the mechanical stability window of these materials.

As UiO-66 exhibits a relatively high thermal,[36,37] mechanical,[28,34,38,39] and chemical stability,[23,36,40] the material can be easily subjected to post-synthetic modification strategies and has been proposed for a wide variety of applications,[3] including hydrogen storage[41] and heterogeneous catalysis.[42,43] The

Received: February 6, 2020
Accepted: March 20, 2020
Published: March 20, 2020

https://dx.doi.org/10.1021/acsmaterialslett.0c00042
ACS Materials Lett. 2020, 2, 438–445

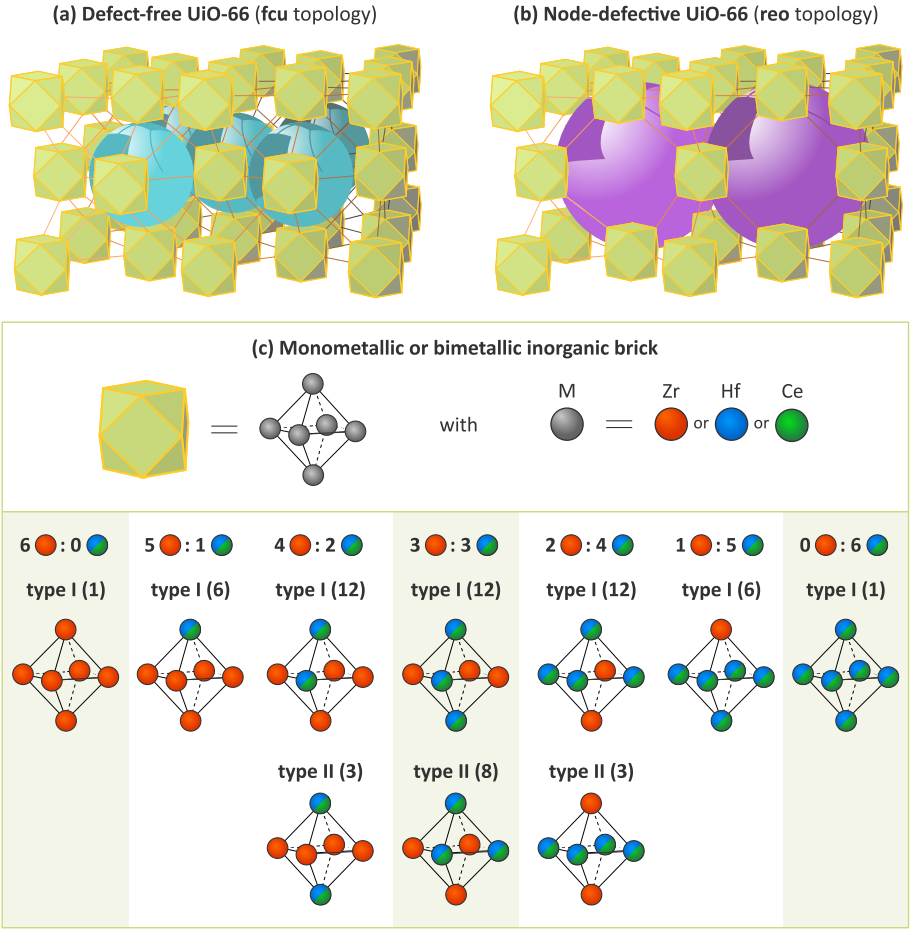

Figure 1. UiO-66(xZr:(6 − x)M) materials discussed in this manuscript. (a) The pristine and (b) the node-defective UiO-66 topologies with largest included spheres. (c) The different inorganic xZr:(6−x)M bricks consisting of x zirconium atoms on the one hand and 6 − x hafnium or cerium atoms on the other hand. The multiplicity of each inorganic brick is given between brackets. The shaded columns indicate those materials that are characterized experimentally.

defect-free UiO-66(Zr) material is composed of 12-fold coordinated $[Zr_6(\mu_3\text{-}O)_4(\mu_3\text{-}OH)_4]^{12+}$ bricks, resulting in the intrinsic **fcu** topology shown in Figure 1a.[44] Experimental UiO-66 samples, however, often contain structural defects in which some of the ligands and even complete inorganic nodes can be missing from the structure,[36,45−50] the latter preferentially ordering into correlated nanodomains adopting the **reo** topology (see Figure 1b).[51] Despite the presence of these defects, which can be largely "ironed out" in UiO-66(Zr) by carefully optimizing the synthesis conditions,[32,47] its outstanding stability makes UiO-66(Zr) an ideal candidate for synthetic or post-synthetic design strategies without appreciably altering the structural integrity of the material.[4,41,52−54] To increase its catalytic activity while still retaining a substantial stability, for instance, mixed-metal UiO-66 materials in which the zirconium ions were partially replaced by either hafnium or cerium ions were designed.[55−59] However, this targeted increase in catalytic activity was observed to come at the expense of a substantial and nonlinear decrease in thermal stability with increasing cerium content, deteriorating from ∼435 °C for UiO-66(Zr) to 220 °C for UiO-66(Ce), thereby undesirably limiting the range of experimental conditions for which the material can be adopted.[60,61] Given the extraordinary research interest in catalytically active UiO-66-type materials, it is crucial to identify whether this reduced stability is an intrinsic effect of UiO-66(Zr:Ce) materials or whether it is rather due to the specific synthesis protocol and can therefore be mitigated by further optimizing the synthesis conditions.

To systematically elucidate the origin of this deteriorated stability and determine its dependence on the metal content of the inorganic brick, we here investigate a series of UiO-66 materials in which the zirconium cations are partially or completely replaced by either hafnium or cerium. This systematic experimental/computational procedure leads to 19 possible inorganic Zr_xCe_{6-x} and Zr_xHf_{6-x} bricks, depicted in Figure 1c. While bimetallic zirconium:cerium materials with varying metal composition were successfully synthesized,[60] these materials were observed to only contain the well-defined Zr_6, Ce_6 and Zr_5Ce_1 bricks in varying ratios.[62] However, as there is no fundamental reason why other bimetallic Zr_xCe_{6-x} bricks would be inaccessible during synthesis, all 19 bricks are retained in this study. Our in situ high-pressure PXRD data, obtained for the three monometallic MOFs and the two bimetallic MOFs with equal amounts of zirconium and either hafnium or cerium, demonstrate that the incorporation of cerium or, to a lesser extent, hafnium ions in UiO-66(Zr) decreases the material's mechanical stability, confirming the earlier observed decrease in thermal stability upon cerium incorporation.[60,61] However, complementary MD simulations at operating conditions, which have been performed for all 19 UiO-66(xZr:(6−x)Ce) and UiO-66(xZr:(6−x)Hf) **fcu** mate-

https://dx.doi.org/10.1021/acsmaterialslett.0c00042
ACS Materials Lett. 2020, 2, 438−445

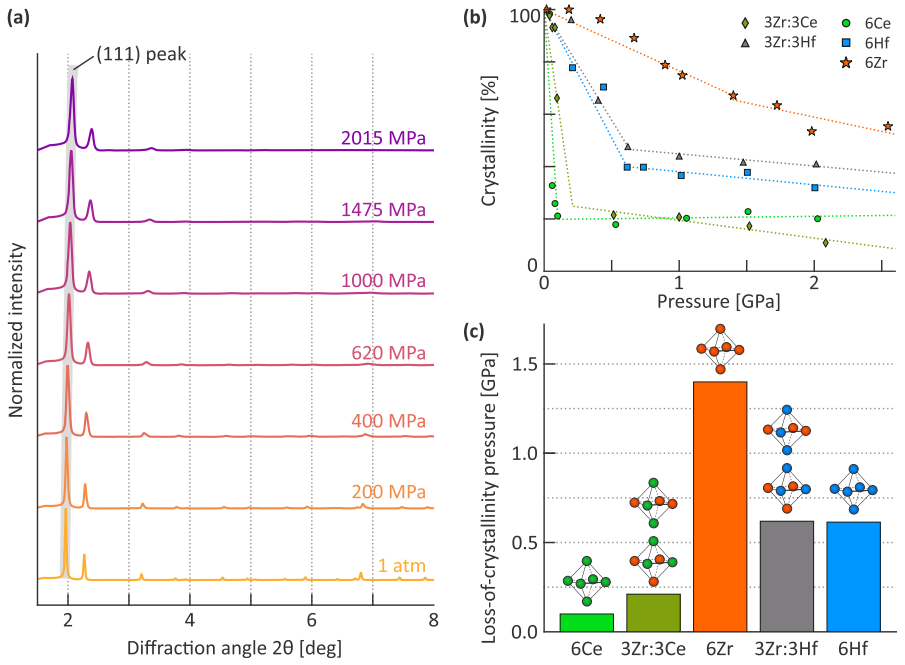

Figure 2. Experimental determination of the loss-of-crystallinity pressure at room temperature. (a). High-pressure powder X-ray diffraction patterns (λ = 0.410344 Å) obtained for the UiO-66(3Zr:3Hf) sample as a function of the applied pressure, with indication of the (111) peak used to determine the crystallinity. (b) Evolution of the crystallinity evaluated from the (111) Bragg reflection peak as a function of the applied pressure for the five experimental UiO-66 samples. Dotted lines are provided as a guide to the eye. (c) Experimental loss-of-crystallinity pressure extracted from the knee in panel b. The data for UiO-66(Zr) was obtained in ref 34.

rials containing one of the brick types in Figure 1c and, additionally, for the three **reo**-defective monometallic MOFs, unequivocally show that only the incorporation of cerium considerably reduces the intrinsic mechanical stability of UiO-66 in a gradual but nonlinear manner, an effect that is absent upon hafnium incorporation. The experimentally observed weaker mechanical stability of the hafnium-containing MOFs with respect to the UiO-66(Zr) sample is found to originate solely from the higher defect content of these samples and can therefore be mitigated by carefully optimizing the synthesis and activation procedures.[32,33]

The five experimental UiO-66 samples (see section S1 for the synthesis procedures) were characterized extensively (see section S2), confirming that MOF crystals consistent with the $Fm\bar{3}m$ space group were obtained.[44] Furthermore, it was verified that the bimetallic UiO-66(3Zr:3Hf) and UiO-66(3Zr:3Ce) samples show the targeted metal-to-metal ratio (see Table S2). For all materials, thermogravimetric analysis indicates that about 33% of the linker positions are unoccupied, except for the monometallic UiO-66(Zr) sample of ref 34, in which only 8.3% of the linker positions are unoccupied due to the optimized synthesis procedure (see Table S3). The in situ PXRD patterns, shown in Figure 2a for UiO-66(3Zr:3Hf) and Figures S13−S17 for all other samples, demonstrate that the diffraction peaks gradually broaden upon increasing pressure but remain consistent with the $Fm\bar{3}m$ space group for pressures up to 2 GPa, indicating that the crystallinity of the materials is reduced at elevated pressures without any phase transition. This loss of crystallinity is most pronounced for the bimetallic UiO-66(3Zr:3Ce) and the monometallic UiO-66(Ce) samples and remains present even after releasing the mechanical pressure again.

To consistently quantify the mechanical resilience of the five samples, their remaining crystallinity at a given pressure is defined based on the broadening of the most prominent diffraction peak of the material, the (111) peak, following the approach outlined in ref 34 for UiO-66(Zr) (see section S1.5). As shown in Figure 2b, two crystallinity regions as a function of the applied pressure can be clearly distinguished for each of the five materials studied here. At low pressures, a rapid decrease in crystallinity with increasing pressure is observed, whereas this decrease is less pronounced or even absent at higher pressures where the solids can be considered as partially amorphous given the substantial broadening of the PXRD peaks with respect to atmospheric pressure.[34] The obtained loss-of-crystallinity pressure, that is, the critical pressure that separates the two regions, is reported in Figure 2c. Whereas an elevated loss-of-crystallinity pressure of ∼1400 MPa was observed earlier for UiO-66(Zr),[34] substituting the zirconium cations by either hafnium or cerium results in an appreciable decrease in mechanical stability. Unexpectedly, both the UiO-66(3Zr:3Hf) and UiO-66(Hf) samples show a reduced loss-of-crystallinity pressure of about 620 MPa despite the chemical similarity of the hafnium and zirconium cations. This effect is even more pronounced when substituting zirconium for cerium as the UiO-66(3Zr:3Ce) and UiO-66(Ce) samples remain stable only for pressures up to ∼210 MPa and ∼100 MPa, respectively, reminiscent of the earlier observed gradual decrease in thermal stability for these materials.[60,61]

While these experimental results demonstrate that substituting the zirconium cations in UiO-66(Zr) by either hafnium or cerium substantially reduces the material's mechanical stability at elevated pressures, the origin of this effect remains unknown at this point. The reduced stability may be intrinsically linked to the hafnium- or cerium-containing inorganic bricks, thereby inherently limiting the conditions under which these materials can be used. Alternatively, it could originate from the increased amount of defects (∼33%) with respect to the zirconium-based

https://dx.doi.org/10.1021/acsmaterialslett.0c00042
ACS Materials Lett. 2020, 2, 438−445

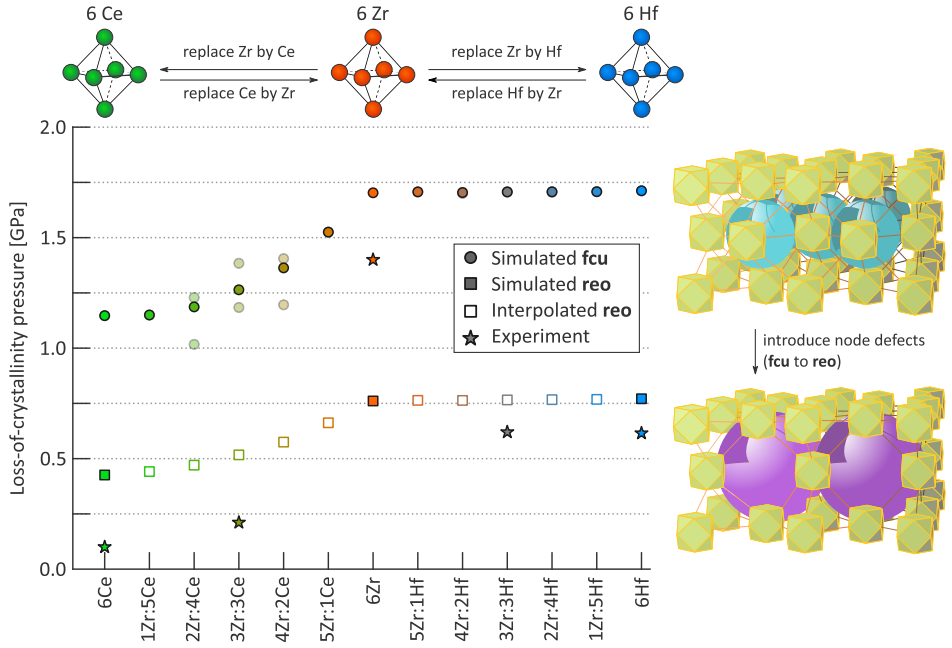

Figure 3. Simulated loss-of-crystallinity pressures at 300 K for all UiO-66 materials as determined from the pressure equations of state, both in the pristine fcu (circles) and node-defective reo (squares) topologies. For those inorganic bricks with two configurations of the metal centers (see Figure 1c), the weighted average is shown, whereas the two independent results are included as semitransparant data points (please note the overlap for the systems with Zr:Hf ratios of 4:2, 3:3, and 2:4). Experimental results are indicated with stars.

material (~8.3%), in which case the synthesis procedure could be optimized to reduce the amount of defects, similar to earlier extensive efforts to iron out the defects in UiO-66(Zr).[32,47]

Given the large amount of synthesis parameters that need to be optimized in order to decrease the defect content of our hafnium- and cerium-containing materials, experimentally isolating the intrinsic stability of these materials is not straightforward. Therefore, fully flexible and system-specific force fields are constructed for the 19 periodic UiO-66 materials containing the inorganic bricks depicted in Figure 1c to isolate the change in intrinsic stability due to the metal substitution. These force fields are derived from ab initio data using the QuickFF protocol for the covalent interactions,[63,64] similar to the approach followed in ref 39. As shown in section S4, good correspondence with both ab initio and experimental structural and mechanical properties is obtained, with a deviation in cell length that does not exceed 1.5 Å. Using these force fields, the loss-of-crystallinity pressure was derived for all 19 **fcu** materials by constructing the pressure-versus-volume equations of state based on MD simulations at 300 K, following the approach outlined in ref 65. As for other UiO-66-type materials,[35,39,66] these pressure equations of state consistently show two distinct regions as a function of the pressure (see section S4.3). In the elastic regime, near the equilibrium volume, the volume decreases linearly with increasing pressure, following Hooke's law. At lower volumes, however, the equation of state deviates from linearity, indicating that the material is deformed plastically. The pressure necessary to bring the material to the critical volume separating both regimes is its computational loss-of-crystallinity pressure, as the symmetry of the crystallographic unit cell would be substantially reduced if the pressure was to be increased further (see section S4.4).

Figure 3 shows the resulting loss-of-crystallinity pressures for all defect-free **fcu** structures (circles), indicating the intrinsic impact of metal substitution on the mechanical stability. For those materials in which the required metal ratio can be obtained by multiple inequivalent inorganic bricks (metal ratios 2:4, 3:3, and 4:2, see Figure 1c), the weighted average of the two inequivalent materials is reported. For the cerium-containing MOFs, a strong and nonlinear decrease in mechanical stability as a function of the cerium content is observed, although less pronounced than the experimental observations. As a result, the intrinsic effect of substituting zirconium by cerium in the inorganic bricks can already partially explain the nonlinear reduction in stability of the experimental UiO-66 samples upon increasing cerium content. In contrast, Figure 3 demonstrates that the chemical similarity between zirconium and hafnium leads to bimetallic UiO-66(Zr:Hf) materials that have a comparable intrinsic stability as the monometallic UiO-66(Zr), indicating that extrinsic effects are fully responsible for the experimentally observed reduction in mechanical stability of the hafnium-containing samples.

Besides the intrinsic mechanical stability of the defect-free materials, the decreased mechanical stability of the experimental hafnium- and cerium-containing samples could also originate from the increased presence of defects with respect to the UiO-66(Zr) sample. For the latter, the synthesis procedure has been extensively optimized.[32] We demonstrated earlier that reducing the inorganic brick coordination in UiO-66(Zr) from 12 to 11 linkers, corresponding with the defect content of our experimental UiO-66(Zr) sample, leads to a reduction in the loss-of-crystallinity pressure from 1.8 GPa to 1.2−1.5 GPa, coinciding with the experimental loss-of-crystallinity pressure of UiO-66(Zr) in Figure 3.[39] Given that the cerium- and hafnium-containing UiO-66 samples are even more defective, we have derived additional force fields for the monometallic UiO-66(Zr), UiO-66(Ce), and UiO-66(Hf) structures containing node defects. These node-defective materials exhibit the **reo** topology postulated by Cliffe et al. and contain the experimentally determined amount of linker vacancies (see

https://dx.doi.org/10.1021/acsmaterialslett.0c00042
ACS Materials Lett. 2020, 2, 438−445

Figure 1b), although the same linker-to-node ratio could in theory also be reached by linker vacancies alone.[51] The pressure-versus-volume equations of state for these node-defective **reo** materials reveal loss-of-crystallinity pressures that are consistently about 0.7−1 GPa lower than the intrinsic mechanical stability observed for the defect-free **fcu** materials. This weakening is largely independent of the metal content of the inorganic brick and can hence be considered as an orthogonal effect to the intrinsic stability.

As demonstrated in Figure 3, this procedure leads to a predicted mechanical stability that approaches the experimental values for all samples. To obtain quantitative agreement between the experimental and computational stabilities reported in Figures 2c and 3, it would be necessary to depart from our assumption that all inorganic bricks in a given material are identical but rather take into account the possibility that different types of inorganic bricks can coexist, as observed in ref 62. However, as the coordination bonds between the inorganic bricks and the organic ligands form very local nucleation points for mechanical instability in these materials, the stability of bimetallic materials with multiple inorganic brick types can be assumed to be defined by the stability of the weakest inorganic brick type, which immediately follows from our results in Figure 3. As a result, Figure 3 reveals that the reduced mechanical stability of the experimental UiO-66(3Zr:3Hf) and UiO-66(Hf) samples is not an intrinsic effect but only stems from defect-induced weakening. In addition, defect-induced weakening also further decreases the already lower intrinsic stability of the UiO-66(Ce) and UiO-66(3Zr:3Ce) samples.

In conclusion, we have demonstrated through high-pressure in situ PXRD experiments that incorporating hafnium or cerium in the inorganic bricks of UiO-66(Zr) substantially decreases the mechanical stability of these MOFs. This effect was found to be the most pronounced for the cerium-containing materials, following the same nonlinear trend as a function of the cerium content as their thermal stability.[60,61] To elucidate the origin of this decreased stability and isolate whether this effect is intrinsic or rather due to the different synthesis protocols for the various samples, complementary MD simulations have been performed using ab initio-based flexible force fields. These simulations indicate that the nonlinear decrease in mechanical stability of the cerium-containing samples is an intrinsic effect of the inorganic brick, whereas the zirconium:hafnium ratio does not affect the intrinsic stability of the hafnium-containing MOFs. Furthermore, the increased presence of defects in the UiO-66(Ce), UiO-66(3Zr:3Ce), UiO-66(Hf), and UiO-66(3Zr:3Hf) samples, a result of the highly optimized synthesis protocol for UiO-66(Zr), yields an additional weakening of these experimental samples. This defect-induced weakening, which was found to reduce the stability of the materials by 0.7−1 GPa independent of the content of the inorganic brick, fully accounts for the reduced stability of the hafnium-containing samples and further decreases the stability of the cerium-containing samples in good agreement with the experimental results. This combined experimental/computational approach therefore demonstrates that carefully optimizing the synthesis protocol may lead to designed UiO-66(Zr:Hf) MOFs with an extraordinary mechanical stability similar to UiO-66(Zr), whereas the intrinsic stability of bimetallic UiO-66(Zr:Ce) MOFs rapidly decreases with increasing cerium content, independent of the synthesis protocol. To further bring these bimetallic MOFs to practical applications in, for example, heterogeneous catalysis or sorption, it will be essential to extend these design principles to also account for the lifetime of these materials during the process.

■ ASSOCIATED CONTENT

Supporting Information

The Supporting Information is available free of charge at https://pubs.acs.org/doi/10.1021/acsmaterialslett.0c00042.

Synthesis and experimental characterization of all samples at ambient conditions, high-pressure X-ray diffraction patterns during pressurization and after pressure release and Birch−Murnaghan equations of state, force field derivation and validation based on ab initio-optimized building blocks, computational pressure-versus-volume equations of state, derivation of the loss-of-crystallinity pressures, and symmetry analysis for all monometallic and bimetallic UiO-66 materials (PDF)

■ AUTHOR INFORMATION

Corresponding Authors

Sven M. J. Rogge − *Center for Molecular Modeling (CMM), Ghent University, B-9052 Zwijnaarde, Belgium;* orcid.org/0000-0003-4493-5708; Email: Sven.Rogge@UGent.be

Veronique Van Speybroeck − *Center for Molecular Modeling (CMM), Ghent University, B-9052 Zwijnaarde, Belgium;* orcid.org/0000-0003-2206-178X; Email: Veronique.VanSpeybroeck@UGent.be

Authors

Pascal G. Yot − *Institut Charles Gerhardt Montpellier (ICGM), Université de Montpellier, CNRS, ENSCM, F-34095 Montpellier, France*

Jannick Jacobsen − *Institut für Anorganische Chemie, Christian-Albrechts-Universität zu Kiel, D-24118 Kiel, Germany*

Francesco Muniz-Miranda − *Center for Molecular Modeling (CMM), Ghent University, B-9052 Zwijnaarde, Belgium*

Steven Vandenbrande − *Center for Molecular Modeling (CMM), Ghent University, B-9052 Zwijnaarde, Belgium*

Jonas Gosch − *Institut für Anorganische Chemie, Christian-Albrechts-Universität zu Kiel, D-24118 Kiel, Germany*

Vanessa Ortiz − *Institut Charles Gerhardt Montpellier (ICGM), Université de Montpellier, CNRS, ENSCM, F-34095 Montpellier, France*

Ines E. Collings − *European Synchrotron Radiation Facility, F-38000 Grenoble, France;* orcid.org/0000-0002-9851-2615

Sabine Devautour-Vinot − *Institut Charles Gerhardt Montpellier (ICGM), Université de Montpellier, CNRS, ENSCM, F-34095 Montpellier, France;* orcid.org/0000-0002-3812-7379

Guillaume Maurin − *Institut Charles Gerhardt Montpellier (ICGM), Université de Montpellier, CNRS, ENSCM, F-34095 Montpellier, France*

Norbert Stock − *Institut für Anorganische Chemie, Christian-Albrechts-Universität zu Kiel, D-24118 Kiel, Germany;* orcid.org/0000-0002-0339-7352

Complete contact information is available at: https://pubs.acs.org/10.1021/acsmaterialslett.0c00042

Author Contributions

J.J. and J.G. synthesized the UiO-66 compounds under supervision of N.S. P.G.Y., V.O., and S.D.-V. experimentally

https://dx.doi.org/10.1021/acsmaterialslett.0c00042
ACS Materials Lett. 2020, 2, 438−445

characterized the compounds and performed the in situ high-pressure powder X-ray diffraction experiments with the aid of I.E.C., J.J., and J.G., all under supervision of G.M. S.M.J.R., F.M.-M., and S.V. performed the ab initio simulations, derived the force fields, carried out the molecular dynamics (MD) simulations, and analyzed the MD results under supervision of V.V.S. S.M.J.R wrote the manuscript with contributions of all authors.

Notes

The authors declare no competing financial interest.

Computational data supporting the results of this work are available from the online GitHub repository at https://github.com/SvenRogge/supporting-info or upon request from the authors. The Yaff software used to perform the MD simulations in this manuscript is freely accessible via https://molmod.ugent.be/software/yaff. Representative input and processing scripts are available at https://github.com/SvenRogge/supporting-info.

■ ACKNOWLEDGMENTS

This work is supported by the Fund for Scientific Research Flanders (FWO), the Research Board of Ghent University (BOF), and by the European Union's Horizon 2020 Research and Innovation Programme [ERC Consolidator Grant Agreement 647755—DYNPOR (2015−2020)]. Computational resources (Stevin Supercomputer Infrastructure) and services were provided by Ghent University. The authors want to thank the European Synchrotron Radiation Facility (ESRF, Grenoble, France) and the ID15B beamline for the allocated beam time and their support during the experiments.

■ REFERENCES

(1) Horcajada, P.; Chalati, T.; Serre, C.; Gillet, B.; Sebrie, C.; Baati, T.; Eubank, J. F.; Heurtaux, D.; Clayette, P.; Kreuz, C.; Chang, J.-S.; Hwang, Y. K.; Marsaud, V.; Bories, P.-N.; Cynober, L.; Gil, S.; Férey, G.; Couvreur, P.; Gref, R. Porous Metal−Organic-Framework Nanoscale Carriers as a Potential Platform for Drug Delivery and Imaging. *Nat. Mater.* **2010**, *9*, 172−178.

(2) Furukawa, H.; Ko, N.; Go, Y. B.; Aratani, N.; Choi, S. B.; Choi, E.; Yazaydin, A. Ö.; Snurr, R. Q.; O'Keeffe, M.; Kim, J.; Yaghi, O. M. Ultrahigh Porosity in Metal−Organic Frameworks. *Science* **2010**, *329*, 424−428.

(3) Deria, P.; Gómez-Gualdrón, D. A.; Bury, W.; Schaef, H. T.; Wang, T. C.; Thallapally, P. K.; Sarjeant, A. A.; Snurr, R. Q.; Hupp, J. T.; Farha, O. K. Ultraporous, Water Stable, and Breathing Zirconium-Based Metal−Organic Frameworks with ftw Topology. *J. Am. Chem. Soc.* **2015**, *137*, 13183−13190.

(4) Kaskel, S. *The Chemistry of Metal−Organic Frameworks: Synthesis, Characterization, and Applications*; John Wiley & Sons, 2016.

(5) Maurin, G.; Serre, C.; Cooper, A.; Férey, G. The New Age of MOFs and of Their Porous-Related Solids. *Chem. Soc. Rev.* **2017**, *46*, 3104−3107.

(6) Hönicke, I. M.; Senkovska, I.; Bon, V.; Baburin, I. A.; Bönisch, N.; Raschke, S.; Evans, J. D.; Kaskel, S. Balancing Mechanical Stability and Ultrahigh Porosity in Crystalline Framework Materials. *Angew. Chem., Int. Ed.* **2018**, *57*, 13780−13783.

(7) Wang, P.-L.; Xie, L.-H.; Joseph, E. A.; Li, J.-R.; Su, X.-O.; Zhou, H.-C. Metal−Organic Frameworks for Food Safety. *Chem. Rev.* **2019**, *119*, 10638−10690.

(8) Eddaoudi, M.; Kim, J.; Rosi, N.; Vodak, D.; Wachter, J.; O'Keeffe, M.; Yaghi, O. M. Systematic Design of Pore Size and Functionality in Isoreticular MOFs and Their Application in Methane Storage. *Science* **2002**, *295*, 469−472.

(9) Yaghi, O. M.; O'Keeffe, M.; Ockwig, N. W.; Chae, H. K.; Eddaoudi, M.; Kim, J. Reticular Synthesis and the Design of New Materials. *Nature* **2003**, *423*, 705−714.

(10) Furukawa, H.; Cordova, K. E.; O'Keeffe, M.; Yaghi, O. M. The Chemistry and Applications of Metal−Organic Frameworks. *Science* **2013**, *341*, 1230444.

(11) Yuan, S.; Chen, Y.-P.; Qin, J.-S.; Lu, W.; Zou, L.; Zhang, Q.; Wang, X.; Sun, X.; Zhou, H.-C. Linker Installation: Engineering Pore Environment with Precisely Placed Functionalities in Zirconium MOFs. *J. Am. Chem. Soc.* **2016**, *138*, 8912−8919.

(12) Li, B.; Wen, H.-M.; Zhou, W.; Xu, J. Q.; Chen, B. Porous Metal−Organic Frameworks: Promising Materials for Methane Storage. *Chem* **2016**, *1*, 557−580.

(13) Kang, Z.; Fan, L.; Sun, D. Recent Advances and Challenges of Metal−Organic Framework Membranes for Gas Separation. *J. Mater. Chem. A* **2017**, *5*, 10073−10091.

(14) Li, H.; Wang, K.; Sun, Y.; Lollar, C. T.; Li, J.; Zhou, H.-C. Recent Advances in Gas Storage and Separation Using Metal−Organic Frameworks. *Mater. Today* **2018**, *21*, 108−121.

(15) Wang, S.; Lee, J. S.; Wahiduzzaman, M.; Park, J.; Muschi, M.; Martineau-Corcos, C.; Tissot, A.; Cho, K. H.; Marrot, J.; Shepard, W.; Maurin, G.; Chang, J.-S.; Serre, C. A Robust Large-Pore Zirconium Carboxylate Metal−Organic Framework for Energy-Efficient Water-Sorption-Driven Refrigeration. *Nat. Energy* **2018**, *3*, 985−993.

(16) Rogge, S. M. J.; Bavykina, A.; Hajek, J.; Garcia, H.; Olivos-Suarez, A. I.; Sepúlveda-Escribano, A.; Vimont, A.; Clet, G.; Bazin, P.; Kapteijn, F.; Daturi, M.; Ramos-Fernandez, E. V.; Llabrés i Xamena, F. X.; Van Speybroeck, V.; Gascon, J. Metal−Organic and Covalent Organic Frameworks as Single−Site Catalysts. *Chem. Soc. Rev.* **2017**, *46*, 3134−3184.

(17) Zhu, L.; Liu, X.-Q.; Jiang, H.-L.; Sun, L.-B. Metal−Organic Frameworks for Heterogeneous Basic Catalysis. *Chem. Rev.* **2017**, *117*, 8129−8176.

(18) Kreno, L. E.; Leong, K.; Farha, O. K.; Allendorf, M.; Van Duyne, R. P.; Hupp, J. T. Metal−Organic Framework Materials as Chemical Sensors. *Chem. Rev.* **2012**, *112*, 1105−1125.

(19) Tchalala, M. R.; Bhatt, P. M.; Chappanda, K. N.; Tavares, S. R.; Adil, K.; Belmabkhout, Y.; Shkurenko, A.; Cadiau, A.; Heymans, N.; De Weireld, G.; Maurin, G.; Salama, K. N.; Eddaoudi, M. Fluorinated MOF Platform for Selective Removal and Sensing of SO_2 from Flue Gas and Air. *Nat. Commun.* **2019**, *10*, 1328.

(20) Xu, G.; Nie, P.; Dou, H.; Ding, B.; Li, L.; Zhang, X. Exploring Metal Organic Frameworks for Energy Storage in Batteries and Supercapacitors. *Mater. Today* **2017**, *20*, 191−209.

(21) Vanduyfhuys, L.; Rogge, S. M. J.; Wieme, J.; Vandenbrande, S.; Maurin, G.; Waroquier, M.; Van Speybroeck, V. Thermodynamic Insight into Stimuli-Responsive Behaviour of Soft Porous Crystals. *Nat. Commun.* **2018**, *9*, 204.

(22) Lenzen, D.; Zhao, J.; Ernst, S.-J.; Wahiduzzaman, M.; Inge, A. K.; Fröhlich, D.; Xu, H.; Bart, H.-J.; Janiak, C.; Henninger, S.; Maurin, G.; Zou, X.; Stock, N. A Metal−Organic Framework for Efficient Water-Based Ultra-Low-Temperature-Driven Cooling. *Nat. Commun.* **2019**, *10*, 3025.

(23) Leus, K.; Bogaerts, T.; De Decker, J.; Depauw, H.; Hendrickx, K.; Vrielinck, H.; Van Speybroeck, V.; Van Der Voort, P. Systematic Study of the Chemical and Hydrothermal Stability of Selected "Stable" Metal Organic Frameworks. *Microporous Mesoporous Mater.* **2016**, *226*, 110−116.

(24) Yuan, S.; Feng, L.; Wang, K.; Pang, J.; Bosch, M.; Lollar, C.; Sun, Y.; Qin, J.; Yang, X.; Zhang, P.; Wang, Q.; Zou, L.; Zhang, Y.; Zhang, L.; Fang, Y.; Li, J.; Zhou, H.-C. Stable Metal−Organic Frameworks: Design, Synthesis, and Applications. *Adv. Mater.* **2018**, *30*, 1704303.

(25) Hu, Z.; Sun, Y.; Zeng, K.; Zhao, D. Structure-Failure Resistance of Metal−Organic Frameworks Toward Multiple-Cycle CO_2 Sorption. *Chem. Commun.* **2017**, *53*, 8653−8656.

(26) Tannert, N.; Ernst, S.-J.; Jansen, C.; Bart, H.-J.; Henninger, S. K.; Janiak, C. Evaluation of the Highly Stable Metal−Organic Framework MIL-53(Al)-TDC (TDC = 2,5-thiophenedicarboxylate)

https://dx.doi.org/10.1021/acsmaterialslett.0c00042
ACS Materials Lett. 2020, 2, 438−445

as a New and Promising Adsorbent for Heat Transformation Applications. *J. Mater. Chem. A* **2018**, *6*, 17706−17712.
(27) Czaja, A. U.; Trukhan, N.; Müller, U. Industrial Applications of Metal−Organic Frameworks. *Chem. Soc. Rev.* **2009**, *38*, 1284−1293.
(28) Peterson, G. W.; DeCoste, J. B.; Glover, T. G.; Huang, Y.; Jasuja, H.; Walton, K. S. Effects of Pelletization Pressure on the Physical and Chemical Properties of the Metal−Organic Frameworks $Cu_3(BTC)_2$ and UiO−66. *Microporous Mesoporous Mater.* **2013**, *179*, 48−53.
(29) Bazer-Bachi, D.; Assié, L.; Lecocq, V.; Harbuzaru, B.; Falk, V. Towards Industrial Use of Metal−Organic Framework: Impact of Shaping on the MOF Properties. *Powder Technol.* **2014**, *255*, 52−59.
(30) Rubio-Martinez, M.; Avci-Camur, C.; Thornton, A. W.; Imaz, I.; Maspoch, D.; Hill, M. R. New Synthetic Routes Towards MOF Production at Scale. *Chem. Soc. Rev.* **2017**, *46*, 3453−3480.
(31) Iacomi, P.; Lee, U.-H.; Valekar, A. H.; Chang, J.-S.; Llewellyn, P. L. Investigating the Effect of Alumina Shaping on the Sorption Properties of Promising Metal−Organic Frameworks. *RSC Adv.* **2019**, *9*, 7128−7135.
(32) Shearer, G. C.; Chavan, S.; Bordiga, S.; Svelle, S.; Olsbye, U.; Lillerud, K. P. Defect Engineering: Tuning the Porosity and Composition of the Metal−Organic Framework UiO-66 via Modulated Synthesis. *Chem. Mater.* **2016**, *28*, 3749−3761.
(33) Firth, F. C. N.; Cliffe, M. J.; Vulpe, D.; Aragones-Anglada, M.; Moghadam, P. Z.; Fairen-Jimenez, D.; Slater, B.; Grey, C. P. Engineering New Defective Phases of UiO Family Metal−Organic Frameworks with Water. *J. Mater. Chem. A* **2019**, *7*, 7459−7469.
(34) Yot, P. G.; Yang, K.; Ragon, F.; Dmitriev, V.; Devic, T.; Horcajada, P.; Serre, C.; Maurin, G. Exploration of the Mechanical Behavior of Metal Organic Frameworks UiO-66(Zr) and MIL-125(Ti) and Their NH_2 Functionalized Versions. *Dalton Trans.* **2016**, *45*, 4283−4288.
(35) Rogge, S. M. J.; Waroquier, M.; Van Speybroeck, V. Reliably Modeling the Mechanical Stability of Rigid and Flexible Metal-Organic Frameworks. *Acc. Chem. Res.* **2018**, *51*, 138−148.
(36) Valenzano, L.; Civalleri, B.; Chavan, S.; Bordiga, S.; Nilsen, M. H.; Jakobsen, S.; Lillerud, K. P.; Lamberti, C. Disclosing the Complex Structure of UiO-66 Metal Organic Framework: A Synergic Combination of Experiment and Theory. *Chem. Mater.* **2011**, *23*, 1700−1718.
(37) DeCoste, J. B.; Peterson, G. W.; Jasuja, H.; Glover, T. G.; Huang, Y.-g.; Walton, K. S. Stability and Degradation Mechanisms of Metal−Organic Frameworks Containing the $Zr_6O_4(OH)_4$ Secondary Building Unit. *J. Mater. Chem. A* **2013**, *1*, 5642−5650.
(38) Wu, H.; Yildirim, T.; Zhou, W. Exceptional Mechanical Stability of Highly Porous Zirconium Metal−Organic Framework UiO-66 and Its Important Implications. *J. Phys. Chem. Lett.* **2013**, *4*, 925−930.
(39) Rogge, S. M. J.; Wieme, J.; Vanduyfhuys, L.; Vandenbrande, S.; Maurin, G.; Verstraelen, T.; Waroquier, M.; Van Speybroeck, V. Thermodynamic Insight in the High-Pressure Behavior of UiO-66: Effect of Linker Defects and Linker Expansion. *Chem. Mater.* **2016**, *28*, 5721−5732.
(40) Kandiah, M.; Nilsen, M. H.; Usseglio, S.; Jakobsen, S.; Olsbye, U.; Tilset, M.; Larabi, C.; Quadrelli, E. A.; Bonino, F.; Lillerud, K. P. Synthesis and Stability of Tagged UiO-66 Zr-MOFs. *Chem. Mater.* **2010**, *22*, 6632−6640.
(41) Bambalaza, S. E.; Langmi, H. W.; Mokaya, R.; Musyoka, N. M.; Ren, J.; Khotseng, L. E. Compaction of a Zirconium Metal−Organic Framework (UiO-66) for High Density Hydrogen Storage Applications. *J. Mater. Chem. A* **2018**, *6*, 23569−23577.
(42) Vermoortele, F.; Bueken, B.; Le Bars, G.; Van de Voorde, B.; Vandichel, M.; Houthoofd, K.; Vimont, A.; Daturi, M.; Waroquier, M.; Van Speybroeck, V.; Kirschhock, C.; De Vos, D. E. Synthesis Modulation as a Tool To Increase the Catalytic Activity of Metal−Organic Frameworks: The Unique Case of UiO-66(Zr). *J. Am. Chem. Soc.* **2013**, *135*, 11465−11468.
(43) Canivet, J.; Vandichel, M.; Farrusseng, D. Origin of Highly Active Metal−Organic Framework Catalysts: Defects? Defects! *Dalton Trans.* **2016**, *45*, 4090−4099.
(44) Cavka, J. H.; Jakobsen, S.; Olsbye, U.; Guillou, N.; Lamberti, C.; Bordiga, S.; Lillerud, K. P. A New Zirconium Inorganic Building Brick Forming Metal Organic Frameworks with Exceptional Stability. *J. Am. Chem. Soc.* **2008**, *130*, 13850−13851.
(45) Shearer, G. C.; Forselv, S.; Chavan, S.; Bordiga, S.; Mathisen, K.; Bjørgen, M.; Svelle, S.; Lillerud, K. P. In Situ Infrared Spectroscopic and Gravimetric Characterisation of the Solvent Removal and Dehydroxylation of the Metal Organic Frameworks UiO-66 and UiO-67. *Top. Catal.* **2013**, *56*, 770−782.
(46) Wu, H.; Chua, Y. S.; Krungleviciute, V.; Tyagi, M.; Chen, P.; Yildirim, T.; Zhou, W. Unusual and Highly Tunable Missing-Linker Defects in Zirconium Metal−Organic Framework UiO-66 and Their Important Effects on Gas Adsorption. *J. Am. Chem. Soc.* **2013**, *135*, 10525−10532.
(47) Shearer, G. C.; Chavan, S.; Ethiraj, J.; Vitillo, J. G.; Svelle, S.; Olsbye, U.; Lamberti, C.; Bordiga, S.; Lillerud, K. P. Tuned to Perfection: Ironing Out the Defects in Metal−Organic Framework UiO-66. *Chem. Mater.* **2014**, *26*, 4068−4071.
(48) Øien, S.; Wragg, D.; Reinsch, H.; Svelle, S.; Bordiga, S.; Lamberti, C.; Lillerud, K. P. Detailed Structure Analysis of Atomic Positions and Defects in Zirconium Metal−Organic Frameworks. *Cryst. Growth Des.* **2014**, *14*, 5370−5372.
(49) Trickett, C. A.; Gagnon, K. J.; Lee, S.; Gándara, F.; Bürgi, H.-B.; Yaghi, O. M. Definitive Molecular Level Characterization of Defects in UiO-66 Crystals. *Angew. Chem., Int. Ed.* **2015**, *54*, 11162−11167.
(50) Fang, Z.; Bueken, B.; De Vos, D. E.; Fischer, R. A. Defect-Engineered Metal−Organic Frameworks. *Angew. Chem., Int. Ed.* **2015**, *54*, 7234−7254.
(51) Cliffe, M. J.; Wan, W.; Zou, X.; Chater, P. A.; Kleppe, A. K.; Tucker, M. G.; Wilhelm, H.; Funnell, N. P.; Coudert, F.-X.; Goodwin, A. L. Correlated Defect Nanoregions in a Metal−Organic Framework. *Nat. Commun.* **2014**, *5*, 4176.
(52) Garibay, S. J.; Cohen, S. M. Isoreticular Synthesis and Modification of Frameworks with the UiO-66 Topology. *Chem. Commun.* **2010**, *46*, 7700−7702.
(53) Kandiah, M.; Usseglio, S.; Svelle, S.; Olsbye, U.; Lillerud, K. P.; Tilset, M. Post-Synthetic Modification of the Metal−Organic Framework Compound UiO-66. *J. Mater. Chem.* **2010**, *20*, 9848−9851.
(54) Khabzina, Y.; Dhainaut, J.; Ahlhelm, M.; Richter, H.-J.; Reinsch, H.; Stock, N.; Farrusseng, D. Synthesis and Shaping Scale-up Study of Functionalized UiO-66 MOF for Ammonia Air Purification Filters. *Ind. Eng. Chem. Res.* **2018**, *57*, 8200−8208.
(55) Jakobsen, S.; Gianolio, D.; Wragg, D. S.; Nilsen, M. H.; Emerich, H.; Bordiga, S.; Lamberti, C.; Olsbye, U.; Tilset, M.; Lillerud, K. P. Structural Determination of a Highly Stable Metal−Organic Framework with Possible Application to Interim Radioactive Waste Scavenging: Hf-UiO-66. *Phys. Rev. B: Condens. Matter Mater. Phys.* **2012**, *86*, 125429.
(56) Lammert, M.; Wharmby, M. T.; Smolders, S.; Bueken, B.; Lieb, A.; Lomachenko, K. A.; De Vos, D.; Stock, N. Cerium-Based Metal Organic Frameworks with UiO-66 Architecture: Synthesis, Properties and Redox Catalytic Activity. *Chem. Commun.* **2015**, *51*, 12578−12581.
(57) Hu, Z.; Nalaparaju, A.; Peng, Y.; Jiang, J.; Zhao, D. Modulated Hydrothermal Synthesis of UiO-66(Hf)-Type Metal−Organic Frameworks for Optimal Carbon Dioxide Separation. *Inorg. Chem.* **2016**, *55*, 1134−1141.
(58) Islamoglu, T.; Atilgan, A.; Moon, S.-Y.; Peterson, G. W.; DeCoste, J. B.; Hall, M.; Hupp, J. T.; Farha, O. K. Cerium(IV) vs Zirconium(IV) Based Metal−Organic Frameworks for Detoxification of a Nerve Agent. *Chem. Mater.* **2017**, *29*, 2672−2675.
(59) Bakuru, V. R.; Churipard, S. R.; Maradur, S. P.; Kalidindi, S. B. Exploring the Brønsted Acidity of UiO-66(Zr, Ce, Hf) Metal−

https://dx.doi.org/10.1021/acsmaterialslett.0c00042
ACS Materials Lett. 2020, 2, 438−445

Organic Frameworks for Efficient Solketal Synthesis from Glycerol Acetalization. *Dalton Trans.* **2019**, *48*, 843−847.
(60) Lammert, M.; Glißmann, C.; Stock, N. Tuning the Stability of Bimetallic Ce(IV)/Zr(IV)-Based MOFs with UiO-66 and MOF-808 Structures. *Dalton Trans.* **2017**, *46*, 2425−2429.
(61) Jacobsen, J.; Reinsch, H.; Stock, N. Systematic Investigations of the Transition between Framework Topologies in Ce/Zr-MOFs. *Inorg. Chem.* **2018**, *57*, 12820−12826.
(62) Lomachenko, K. A.; Jacobsen, J.; Bugaev, A. L.; Atzori, C.; Bonino, F.; Bordiga, S.; Stock, N.; Lamberti, C. Exact Stoichiometry of Ce_xZr_{6-x} Cornerstones in Mixed-Metal UiO-66 Metal−Organic Frameworks Revealed by Extended X-ray Absorption Fine Structure Spectroscopy. *J. Am. Chem. Soc.* **2018**, *140*, 17379−17383.
(63) Vanduyfhuys, L.; Vandenbrande, S.; Verstraelen, T.; Schmid, R.; Waroquier, M.; Van Speybroeck, V. QuickFF: A Program for a Quick and Easy Derivation of Force Fields for Metal−Organic Frameworks from Ab Initio Input. *J. Comput. Chem.* **2015**, *36*, 1015−1027.
(64) Vanduyfhuys, L.; Vandenbrande, S.; Wieme, J.; Waroquier, M.; Verstraelen, T.; Van Speybroeck, V. Extension of the QuickFF Force Field Protocol for an Improved Accuracy of Structural, Vibrational, Mechanical and Thermal Properties of Metal−Organic Frameworks. *J. Comput. Chem.* **2018**, *39*, 999−1011.
(65) Rogge, S. M. J.; Vanduyfhuys, L.; Ghysels, A.; Waroquier, M.; Verstraelen, T.; Maurin, G.; Van Speybroeck, V. A Comparison of Barostats for the Mechanical Characterization of Metal−Organic Frameworks. *J. Chem. Theory Comput.* **2015**, *11*, 5583−5597.
(66) Moghadam, P. Z.; Rogge, S. M. J.; Li, A.; Chow, C.-M.; Wieme, J.; Moharrami, N.; Aragones-Anglada, M.; Conduit, G.; Gomez-Gualdron, D. A.; Van Speybroeck, V.; Fairen-Jimenez, D. Structure-Mechanical Stability Relations of Metal−Organic Frameworks via Machine Learning. *Matter* **2019**, *1*, 219−234.

https://dx.doi.org/10.1021/acsmaterialslett.0c00042
ACS Materials Lett. 2020, 2, 438−445